MRS Advances © 2016 Materials Research Society
DOI: 10.1557/adv.2016.224

Synthesis of Transparent Semiconducting Metal-oxides via Polymeric Precursor Route for Application in Thin-film Field-Effect Transistors

Cleber A. Amorim[1], Giovani Gozzi[1], Dante L. Chinaglia[1], Francisco José dos Santos[1] and Lucas Fugikawa Santos[1,2]

[1] Departamento de Física, Univ Estadual Paulista - UNESP, Av. 24A, 1515, CEP: 13500-970,Rio Claro, SP, Brazil.
[2] Departamento de Física, Univ Estadual Paulista - UNESP, R. Cristovao Colombo 2265, CEP 15054-000, São José do Rio Preto, SP, Brazil.

ABSTRACT

Solution-processed zinc oxide (ZnO) thin-film transistors (TFTs) obtained via hydrolysis/pyrolysis of an organic precursor present an excellent technique to obtain high performance electronic devices with low manufacturing cost. In the current work, we propose the use of an alternative deposition method, based on a polymeric precursor route (known as Pechini), to obtain solution-processed ZnO compact films as the active layer of TFTs. The elimination of the organic phase and the formation of inorganic thin-films was carried out by thermal treatment at different temperatures (ranging from 200ºC to 500ºC) and at different times (from 5 min to 2 hours), being monitored by UV-vis and infrared (IR) optical absorption spectroscopy. It was observed that, for temperatures above 400ºC and treatment times superior to 30 min, the organic phase was completely eliminated, remaining only the inorganic (metal oxide) phase. The optical bandgap of the resulting ZnO films, determined from UV-vis absorption, is about 3.4 eV. The electrical characteristics (output and transfer curves) of the obtained devices demonstrate the feasibility of Pecchini method to build solution-processed metal oxide TFTs. The results for the electrical mobility of the majority charge-carriers (electrons) and for the threshold voltage were 0.39 $cm^2.V^{-1}.s^{-1}$ and 0.45 V, respectively.

INTRODUCTION

Transparent semiconducting metal-oxides like zinc oxide (ZnO) and other tertiary and quarternary compounds have been widely used as active layer of thin-film transistors (TFTs) envisaging applications in large-area active matrix displays (AMDs) or totally transparent circuitry due to their considerably high charge-carrier mobility, optical transparency and stability [1]. Latest advances on this technology permitted the achievement of charge carrier mobilities considerably higher (up to 100 $cm^2V^{-1}.s^{-1}$) than the mobility of amorphous Si (*ca*. 1 $cm^2V^{-1}.s^{-1}$), which is the most currently used active material in AMDs. Higher mobilities make possible the fabrication of larger displays, with higher resolution and higher scanning frequencies, which are crucial for an increasingly more demanding market. Moreover, the use of transparent metal oxides as electrodes, active and dielectric materials of TFTs allows the production of totally transparent devices and displays, which has a striking appeal for innovative applications.

Recently, TFTs comprising solution-processed metal oxides obtained via hydrolysis/pyrolysis of an organic precursor [2-9] have achieved electrical performance which challenges metal-oxide TFTs produced by traditional deposition methods (e.g. RF sputtering), presenting attractive characteristics as low manufacturing cost and possibility to cover large-areas. However, solution-processed metal oxide thin films still suffer from

undesirable characteristics such as film non-uniformity, high porosity and unstable electrical response. In order to circumvent these problems, we have used an alternative method based on a polymeric precursor route [10-12] (Pechini) to obtain more compact and uniform metal oxide films via solution processing. The films were fabricated by spin-coating deposition and characterized by optical absorption spectroscopy (UV-vis and FTIR) and by thermal analysis (TGA and DTA). Electrical measurements (d.c. current-voltage) demonstrate that it was possible to successfully use Pechini method to fabricate TFTs with a ZnO active layer.

MATERIALS AND METHODS

Transistor preparation

The substrates of the fabricated TFTs comprise *p*-type (Boron) Silicon wafers (500 μm thick) with a thermally grown SiO_2 layer (200 nm thick), purchased from Microchemicals GmbH. A thin aluminum layer (500 nm thick) was deposited, by sputtering, onto the rear surface (opposite to the SiO_2 layer) to improve the contact of the gate electrode to external circuit. The bottom-gate, bottom-contact TFT structure was defined by photolithographic process (lift-off), using interdigitate electrodes as drain and source, deposited on top of the SiO_2 dielectric layer. These electrodes were composed by a Cr adhesion bottom layer (10 nm) and a contact top layer of Au (50 nm), both deposited by sputtering. TFT fabrication was concluded by spin-coating the polymeric precursor solution onto the previously patterned, cleaned and treated Si/SiO_2 substrates.

The polymeric precursor solution was prepared via Pechini method [10-12] using zinc acetate dehydrate (Sigma Aldrich), $Zn(CH_3\ COO)_2\ 2H_2O$, as Zn source. The processing solution was obtained by mixing two previously prepared solutions: solution A, prepared by dissolving 50 mg of zinc acetate in 208 mg of ethanol and 152 mg of nitric acid; and solution B, prepared by dissolving 50 mg of citric acid in 39 mg of ethylene glycol. Solution A was homogenized at room temperature whereas solution B was heated up to 80 °C, both under constant stirring and during 30 min. Afterwards, both solutions were mixed and the resulting solution was cooled down to room temperature and was ready to be deposited.

Prior to film deposition, the Si/SiO_2 patterned substrates were cleaned and treated in a sequence process: i) sonication for 20 min, at 60 ^oC, in a 5% Alconox® (Sigma Aldrich) water solution; ii) abundantly rinsed with deionized water; iii) dried with jet of dry clean air; iv) sonication for 20 min, at room temperature, in pure acetone; v) dried with jet of dry clean air; vi) heated up to 120 ^oC in an oven, for 5 min and vi) oxygen RF plasma cleaning for 5 min. The polymeric precursor solution was deposited by spin coating (2000 rpm for 30 s). After deposition, the films were dried at 200 °C, for 30 min, in air, for solvent evaporation, on a hot plate. Subsequently, the temperature was raised up to 350 °C, remained still for 30 min, and raised again up to 500 °C, and remained still for more 30 minutes. The heating rate was 10 °C/min.

Characterization techniques

Samples for TGA and DTA were prepared by dispensing 18 mg of the polymeric precursor solution into an aluminum pan, which were heated up to 80 ^oC in an oven, during 2 hours, in order to evaporate any reaction residues. The thermographic analysis (TGA) and differential thermal analysis (DTA) were performed using Shimadzu equipments, models TGA50 and DTA50, respectively. The measurements were performed using dry air as a carrier, and the temperature ramps were performed using a 5°C/min rate, in the 20 °C up to 500 °C temperature range.

For UV-Vis characterization, the films were deposited onto quartz substrates, following the same previously described cleaning and treatment procedures used for the Si/SiO_2 substrates. Spin coating deposition (2000 rpm, 30 s) was followed by heating up the substrate up to 200 ^oC, in air, for 30 min. Different samples were produced by further heating the substrates at different temperatures (300 °C, 400 °C and 500 °C) during 30 minutes, to observe spectroscopy variations due to the thermal treatment. A Varian-Cary 50 spectrophotometer, operating in the 300 nm to 800 nm wavelength range, was employed in all the experiments.

The samples for FTIR (ATR mode) measurements were deposited onto gold (100 nm thick) covered glass substrates, which were cleaned and treated according to the same procedure used to clean the quartz and Si/SiO_2 substrates. Film deposition and thermal treatment at different temperatures followed the same process than the samples used for UV-Vis analysis. A Thermo Nicolet 6700 FTIR spectrometer, in the wave number range between 4000 cm^{-1} and 500 cm^{-1}, was used to perform the experiments.

Electrical characterization (output and transfer curves) of the transistors were carried out at room temperature, using a Keithley 6517A electrometer to measure the channel current and to apply the voltage between source and drain electrodes (V_{DS}) as well. The gate voltage (V_G) was supplied by a Keithley 2401 source-measure unit. Capacitance-voltage measurements were carried out using a Solartron SI 1260 frequency response analyzer.

RESULTS AND DISCUSSION

Figure 1 shows the thermogravimetric analysis of the polymeric precursor material obtained using the experimental procedure described above. From room temperature up to 150^{o}C, one observes a small mass loss due to an endothermic process (Fig. 1-b). Such loss can be attributed to evaporation of acetic acid residues. Around 150^{o}C, a rise in the mass loss rate occurs, associated to an endothermic process (Fig. 1-b). Between 200^{o}C and 250^{o}C, the mass loss rate becomes constant and the accumulated loss is about 20% of the total mass. For temperatures above 250^{o}C another mass loss process occurs, associated to an endothermic process, with maximum mass loss rate around 300^{o}C. This process continues until about 400^{o}C, where 84% of the total mass of the polymeric precursor is lost. Further heating reveals another endothermic process, with discrete mass loss (about 16% of the total mass), between 450^{o}C and 500^{o}C, peaking around 470^{o}C. In the DTA curve, in this range, one observes an exoenergetic peak superimposed to the endoenergetic peak associated to the mass loss process. This exoenergetic process corresponds to the zinc oxide crystallization.

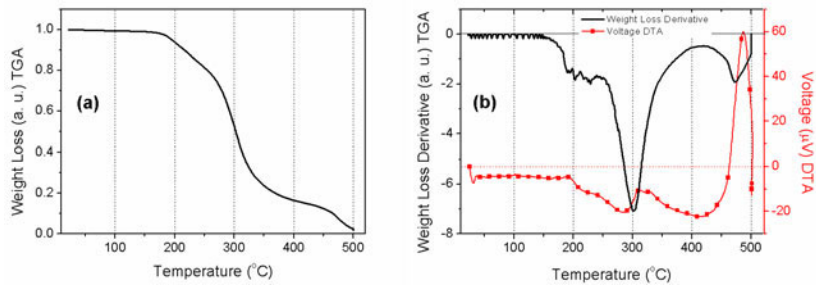

Figure 1: Thermogravimetric mass loss curve (a) and differential mass loss curve (b) of polymeric precursor films used to produce ZnO TFTs.

Figura 2 refers to the FTIR spectra from films exposed to different thermal treatments (300ºC, 400ºC and 500ºC). Each sample was treated at temperatures superior to each of the three mass loss processes identified from the thermal analysis. The main peaks, corresponding to 11 vibrational modes of different chemical groups of the polymeric precursor are presented on Table I.

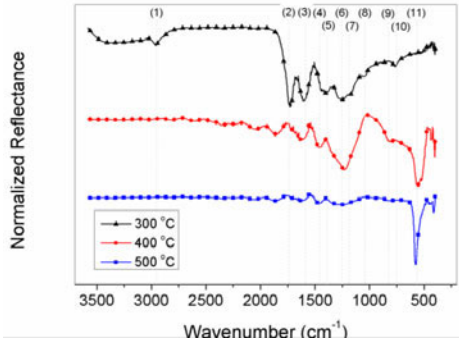

Figure 2: FTIR spectra of the polymeric precursor films treated at different temperatures.

For the sample treated at 300ºC, peaks from (1) to (8) (assigned in Figure 2) are present in the FTIR spectrum, which corresponds to vibrational modes of chemical groups associated to zinc hydroxide (Table I). The spectrum of the sample treated at 400ºC shows the suppression of peaks (1), (2), (5) and (8), related to the esther group, and the up arising of peaks (9), (10) and (11), corresponding to zinc hydroxide and zinc oxide, respectively. For the sample treated at 500ºC, the only remaining peak is (11), demonstrating that all the organic phase from the initial polymeric precursor was eliminated. These results show that the first two mass loss processes corresponds to the break of the esther molecules and of the zinc chelate. For the first mass loss process (below 350ºC), groups with lower binding energy, like OH groups and C=O groups, are broken and eliminated by evaporation.

Table I: Association of the peaks from the FTIR spectra for films treated at different temperatures.

Peak	Wavenumber (cm^{-1})	Vibrational mode	Temperature (ºC)		
			300	400	500
(1)	2947	OH stretch (esther)	X		
(2)	1737	C=O stretch (esther)	X		
(3)	1593	H-C-H bend (esther and zinc chelate)	X	X	
(4)	1454	H-C-H bend (esther and zinc chelate)	X	X	
(5)	1388	C-H rock in plane on CHO (esther)	X		
(6)	1255	CO Stretch (esther)	X	X	
(7)	1188	C-O stretch (zinc chelate)	X	X	
(8)	1044	C-COH stretch (esther)	X		
(9)	825	Zn-OH		X	
(10)	751	Zn-OH	X	X	
(11)	567	Zn-O		X	X

The UV-Vis spectra obtained for samples treated at 300ºC, 400ºC and 500ºC are depicted in Figure 3-a. The derivative of the spectra, used to determine the optical bandgap

energy, are shown in Figure 3-b. For the sample treated at 300ºC, it is not possible to determine the optical bandgap, which means that the amount of ZnO formed at this temperature is not significant compared to the amount of organic material remaining in the film. Treating the sample at 400ºC causes a slight inflexion in the absorption curve, which is associated to the optical bandgap of ZnO, overlaid with the optical absorption spectrum of the zinc chelate. The sample treated at 500ºC presents a very clear absorption edge around 3.3 eV, which is the expected energy for the ZnO bandgap, corroborating the thermal analysis and FTIR results.

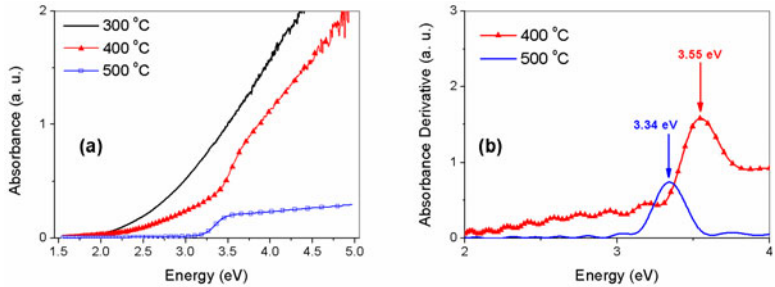

Figure 3: UV-vis spectra of the polymeric precursor films treated at different temperatures (a). Determination of the optical bandgap for films treated at different temperatures (b).

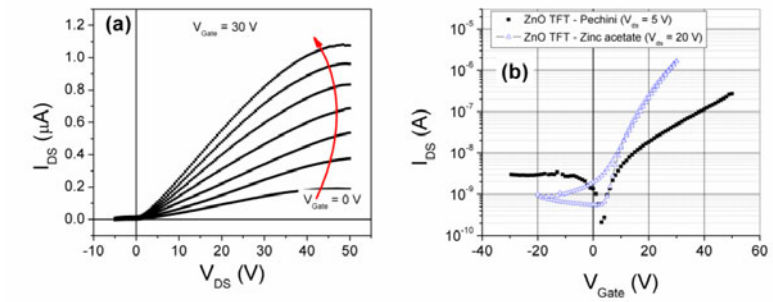

Figure 4: Output (a) and transfer (b) curves obtained for a ZnO TFT in a bottom-gate, bottom-contact structure, after a 400ºC treatment.

The d.c. electrical characterization of a TFT transistor made from a Si/SiO_2 patterned substrate treated at 500ºC is presented in Fig. 4-a (output curve) and Fig. 4-b (transfer curve). The characteristic behavior, as expected, is for a n-type semiconductor layer, with clear saturation and modulation features in spite of a quite high intrinsic (V_G = 0 V) current. The transfer curve presents a on/off ratio of at about 10^2. From the transfer curve, it was also possible to determine (from the slope and intersection of the curve of the square root of I_D *vs.* V_G) the charge-carrier mobility (about 0.39 $cm^2.V^{-1}.s^{-1}$) in the saturation regime and the device threshold voltage ($V_{th} \approx$ 0.45 V). Fig. 4-b also presents, for comparison, the transfer curve of a solution-processed ZnO TFT made by directly dissolving zinc acetate in 2-methoxyethanol, without formation of the polymeric precursor. This device presents a slightly higher mobility in the saturation regime (0.48 $cm^2.V^{-1}.s^{-1}$) and better on/off ratio (>10^3), in spite of a little higher threshold voltage ($V_{th} \approx$ 3.1 V).

In order to confirm that the films obtained from Pechini method were more compact than the produced from pure zinc acetate solutions, capacitance-voltage measurements of ZnO films on top of the Si/SiO_2 substrates were performed in MIS capacitor structures ($Al/ZnO/SiO_2/p$-Si/Al) using both deposition techniques. The average evaluated capacitance per unit area of films formed from zinc acetate solution was about 92 nF/cm^2 against 112 nF/cm^2 for films deposited by Pechini method, which can be attributed to a denser ZnO active layer.

CONCLUSIONS

Thin-films of ZnO were successfully produced by using the polymeric precursor method (Pechini) and applied to the construction of thin-film field effect transistors. Thermal analysis, FTIR and UV-Vis spectroscopy have shown that pure ZnO films, with an optical bandgap of 3.3 eV could be achieved only at temperatures around 500ºC. Although the performance of the TFTs produced via Pechini method was not superior to TFTs produced by deposition of zinc acetate, results from capacitance measurements indicated that the films formed using the polymeric precursor route may present a more compact structure, which can be an advantage to achieve better device stability. Further improvements in the solution preparation and in the processing methods would probably improve the device performance and decrease the temperature treatment necessary to obtain films with characteristic field-effect response and compactible to flexible substrates.

ACKNOWLEDGMENTS

The authors would like to acknowledge financial support from FAPESP (research grants 2013/24461-7 and 2008/57706-4) and technical support from CNPEM (research proposals LMF-19181 and LMF-14135).

REFERENCES

1. T. Kamiya, K. Nomura and H. Hosono, *Sci. Technol. Adv. Mater.* **11**, 044305 (2010).
2. E. Fortunato, P. Barquinha and R. Martins, *Adv. Mater.* DOI: 10.1002/adma.201103228 (2011).
3. Y. J. Kim, S. Oh, B. S. Yang, S. J. Han, H. W. Lee, H. J. Kim, J. K. Jeong, C. S. Hwang and H. J. Kim, *ACS Applied Materials & Interfaces* **6**, 14026-14036 (2014).
4. W. J. Lee, W. T. Park, S. Park, S. Sung, Y. Y. Noh and M. H. Yoon, *Adv. Mater.* DOI: 10.1002/adma.201502239 (2015).
5. C. S. Li, Y. N. Li, Y. L. Wu, B. S. Ong and R. O. Loutfy, *J. Phys. D: Appl. Phys.* **41**, 125102 (2008).
6. T. O. L. Sunde, E. Garskaite, B. Otter, H. E. Fossheim, R. Saeterli, R. Holmestad, M. A. Einarsrud and T. Grande, *J. Mater. Chem.* **22**, 15740 (2012).
7. S. A. Kamaruddin, K. Y. Chan, H. K. Yow, M. Z. Sahdan, H. Saim and D. Knipp, *Appl. Phys. A* **104**, 263-268 (2011).
8. K. H. Kim, G. H. Kim and H. J. Kim, *Phys. Status Solidi* **207** 1660-1663 (2010).
9. K. K. Banger, Y. Yamashita, K. Mori, R. L. Peterson, T. Leedham, J. Rickard and H. Sirringhaus, *Nature Materials* DOI: 10.1038/NMAT2914 (2010).
10. C. Sánchez, J. Doria, C. Paucar, M. Hernandez, A. Mósquera, J. E. Rodríguez, A. Gómez, E. Baca and O. Morán, *Physica B* **405**, 3679-3684 (2010).
11. G. He, J. H. Cai, G. Ni, *Mater. Chem. Phys.* **110** 110-114 (2008).
12. M. P. Pechini, US Patent 3330697 (July 11, 1967).